ISSN 1070-3284, Russian Journal of Coordination Chemistry, 2022, Vol. 48, No. 3, pp. 164–172. © The Author(s), 2022. This article is an open access publication.
Russian Text © The Author(s), 2022, published in Koordinatsionnaya Khimiya, 2022, Vol. 48, No. 3, pp. 168–177.

Tetranuclear Hydroxo Complexes of Rare-Earth Elements with the Cubane Core as Products of Self-Controlled Hydrolysis

D. M. Tsymbarenko[a], *, D. I. Grebenyuk[a], M. A. Burlakova[a], and A. S. Shurkina[a]

[a] *Moscow State University, Moscow, 119992 Russia*

**e-mail: tsymbarenko@inorg.chem.msu.ru*

Received April 26, 2021; revised August 16, 2021; accepted August 18, 2021

Abstract—Tetranuclear hydroxo complexes $[La_4(Deta)_4(OH)_4(Tfa)_3(DetadcH)_2](HTfa)(H_2O)_7(Tfa)_3$ (**I**) and $[Nd_4(Deta)_4(OH)_4(Tfa)_3(DetadcH)_2](H_2O)_n(Tfa)_3$ (**II**) with diethylene-*N*,*N*'-dicarbamate anions ($DetadcH^-$) are synthesized for the first time by the reactions of lanthanum trifluoroacetate and neodymium trifluoroacetate with a solution of diethylenetriamine (Deta) in air under the self-controlled hydrolysis conditions and are characterized by X-ray diffraction, powder X-ray diffraction, IR spectroscopy, and elemental analysis. Compounds **I** and **II** contain the same-type complex cationic fragment with the cubane metal–oxygen core stabilized due to four chelate Deta ligands and two bridging $DetadcH^-$ ligands. The DFT calculations of the geometry and vibrational spectrum of the $[La_4(Deta)_4(OH)_4(Tfa)_3(DetadcH)_2]^{3+}$ complex cation are performed.

Keywords: rare-earth elements, polynuclear complexes, carboxylates, carbamate, crystal structure

DOI: 10.1134/S1070328422030058

INTRODUCTION

Polynuclear complexes of rare-earth elements (REE) attract attention of researchers as promising compounds for the production of luminescent and magnetic materials. A close arrangement of several REE ions in one molecule can provide an energy transfer between them, which is important for manufacturing new luminescent thermometers [1], luminescent sensors [2], and up-conversion [3] and magnetocaloric [4, 5] materials. Similar structural properties of elements in the REE series and different luminescence and magnetic properties determined by the number of *f* electrons provide a possibility for fine tuning of functional properties of the obtained material. Molecular clusters of REE have been considered in the recent years as secondary structural blocks for new coordination polymers, including metal-organic frameworks [6].

Additional interest in systems of REE carboxylates with amines is also caused by their application as precursors in the solution method for the preparation of inorganic thin-film materials based on REE: oxides and fluorides [7–10]. An important advantage of these systems is a slight hydrolysis under the action of amines to form an amorphous gel providing upon annealing the homogeneity and uniformity of the formed film of inorganic material. However, a tendency to gel formation impedes, in most cases, the isolation of intermediate complexes in the crystalline state and the study of their structures by X-ray diffraction (XRD).

In acidic aqueous solutions REE ions exist as aquated ions $[Ln(H_2O)_n]^{3+}$ (n = 8, 9). Their stepwise hydrolysis occurs with increasing pH to form hydroxo complexes of REE and finally the corresponding hydroxide $Ln(OH)_3$ at pH from 7.5 (La) to 5.7 (Lu) [11]. At the same time, the presence of anionic or neutral chelating ligands in a solution can prevent the full condensation of the hydroxo complexes to $Ln(OH)_3$ resulting in the formation of molecular clusters of REE.

A variety of polynuclear molecular clusters of REE with different numbers of metal atoms was described [12]. Among them the most studied are the tetranuclear clusters based on the cubane fragment $\{Ln_4(\mu_3\text{-}OH)_4\}$ [13, 14] and planar fragment $\{Ln_4(\mu_3\text{-}OH)_2\}$ [15, 16], as well as the hexanuclear octahedral clusters based on the $\{Ln_6(\mu_3\text{-}OH)_8\}$ fragment [17–19]. The main method for the synthesis of molecular clusters of REE is the controlled hydrolysis of an inorganic salt of REE in the presence of an organic ligand that stabilizes the cluster and prevents its further condensation. This method makes it possible to obtain diverse polynuclear architectures containing the complexes with amino acids [20], Schiff bases [21], and diketones [22, 23].

We have previously reported the two-step synthesis of the octahedral molecular clusters of REE including

the controlled hydrolysis step in the presence of the pivalate anion leading to the formation of 1D coordination polymers containing the planar $\{Ln_4(\mu_3\text{-}OH)_2\}$ core [24] and subsequent introduction of the chelating neutral diethylenetriamine ligand that deepens the hydrolysis and stabilizes the octahedral architecture due to hydrogen bonds with the pivalate anions [17].

The synthesis, crystal structures, and quantum chemical simulation of new tetranuclear molecular clusters of La and Nd trifluoroacetates with diethylenetriamine and diethylenetriamine-*N*,*N*'-dicarbamate anion are reported in this work.

EXPERIMENTAL

The following starting reagents were used: $La_2(CO_3)_3{\cdot}6H_2O$ (reagent grade), $Nd_2(CO_3)_3{\cdot}6H_2O$ (reagent grade), trifluoroacetic acid (HTfa, P&M Invest, 98%), diethylenetriamine (Deta, Sigma-Aldrich, 99%), and isopropyl alcohol (reagent grade). All syntheses were carried out in air in glass beakers.

Lanthanum and neodymium trifluoroacetate hydrates $Ln(Tfa)_3(H_2O)_3$ (Ln = La, Nd) were synthesized using a known procedure from $Ln_2(CO_3)_3{\cdot}6H_2O$ [10]. The purity of the products was confirmed by XRD and thermogravimetric analysis. The yield was ~95%.

Synthesis of polynuclear hydroxo complexes $[Ln_4(Deta)_4(OH)_4(Tfa)_3(DetadcH)_2]^{3+}(Tfa)^-_3{\cdot}nH_2O{\cdot}m$HTfa (Ln = La (I), Nd (II)). A weighed sample of $Ln(Tfa)_3(H_2O)_3$ (0.7 mmol) was dispersed in isopropyl alcohol (5 mL), and Deta (1.4 mmol, 0.151 mL) was added with stirring. The reaction mixture was stirred at 60°C until a transparent solution was obtained. Then the solution was cooled slowly and left to stay in an open beaker to evaporate the solvent with slow crystallization. Fine plate-like crystals were found after 3 days on the walls and bottom of the beaker. Few colorless crystals of compound **I** were obtained in the volume of the gel-like hydrolysis product for Ln = La. Pale purple crystals of compound **II** were obtained as the major product for Ln = Nd. The yield was 60%.

For $C_{42}H_{95}N_{18}O_{33}F_{21}La_4$ (**I**)			
Anal. calcd., %	C, 21.6	H, 4.1	N, 10.8
Found, %:	C, 21.9	H, 4.2	N, 11.1
For $C_{40}H_{82}N_{18}O_{25}F_{18}Nd_4$ (**II**)			
Anal. calcd., %	C, 22.5	H, 3.9	N, 11.8
Found, %:	C, 22.3	H, 4.2	N, 11.5

IR (ν, cm^{-1}): 3368 m, 3309 m $\nu_{as}(NH_2)$; 3100 w $\nu_{as}(CH_2)$; 2952 w, 2920 w, 2876 m $\nu_s(CH_2)$; 1688 s, 1673 s $\nu_{as}(COO^-)$; 1620 sh $\delta(NH_2)$; 1596 s $\delta(NH_2)$ + $\nu_{as}(-NH-COO)$; 1490 s $\nu_s(-NH-COO)$; 1454 m $\delta(CH_2)$ + $\nu_s(COO-)$; 1428 m $\delta(CH_2)$ + $\nu_{as}(-NH-COO)$; 1396 m $\delta_w(CH_2{}^{DetadcH-})$; 1339 m $\delta_r(C-NH-C)$ + $\delta_w(CH_2)$; 1199 s, 1178 s, 1127 s ν(CF); 959 m, 923 m, 829 m, 799 s, 716 s, 591 m.

Analyses to C, H, and N were carried out on an Elementar Vario Micro Cube microanalyzer. The IR spectrum of powdered compound **II** was recorded in the attenuated total reflectance (ATR) mode on a Shimadzu IRAffinity-1S spectrometer in the range of wave numbers from 500 to 4000 cm^{-1}. Powder XRD of compound **II** was carried out on a Rigaku Miniflex 600 diffractometer (CuK_α radiation, K_β filter, D/teX Ultra detector) in the Bragg–Brentano geometry.

Single crystal XRD was carried out on a Bruker D8 Quest diffractometer (MoK_α radiation, λ = 0.71073 Å) equipped with a Photon III detector at 100 K. All crystals of compounds **I** and **II** demonstrated broad diffraction maxima with the fast angular decay of intensity, and the diffraction data acquisition was performed with an exposure duration of 60 s/frame. The structures were solved by direct methods with subsequent Fourier syntheses and refined by full-matrix least squares. All non-hydrogen atoms (except for atoms of the disordered out-of-sphere trifluoroacetate anions and water molecules in compound **I**) were refined in the anisotropic approximation. Hydrogen atoms were introduced into the calculated positions (from geometric concepts and concepts of hydrogen bond formation) and refined by the riding model with fixed isotropic thermal parameters. All calculations were performed using the SHELXL 2017 software [25]. An absorption correction was applied using the SADABS program [26]. Selected crystallographic parameters are given in Table 1.

The full set of crystallographic parameters for the structures of compounds **I** and **II** was deposited with the Cambridge Crystallographic Data Centre (CIF files CCDC nos. 2077216 and 2077217, respectively; deposit@ccdc.cam.ac.uk; http://www.ccdc.cam.ac.uk/data_request/cif).

Quantum chemical simulation was performed for the isolated cationic fragment $[La_4(Deta)_4(OH)_4(Tfa)_3(DetadcH)_2]^{3+}$ using the FireFly 8.2 software [27] in the framework of the density functional theory (DFT) with the PBE0 functional and 6-31G* basis sets for C, F, O, N, and H atoms and quasi-relativistic effective Stuttgart–Cologne large-core potential (ECP46MWB) and corresponding basis set for La [28, 29]. The initial geometry of the cationic fragment was built on the basis of the XRD data and then optimized without symmetry restraints. The optimized geometry was verified to the absence of imaginary frequencies in the calculated vibrational spectrum.

Table 1. Results of crystal structure refinement

Parameter	Value	
	I	**II**
Formula	$C_{42}H_{95}N_{18}O_{33}F_{21}La_4$	$C_{40}H_{82}N_{18}O_{25}F_{18}Nd_4$
FW	2334.99	2134.19
Crystal system	Monoclinic	Triclinic
Space group	$C2/c$	$P\bar{1}$
a, Å	28.147(3)	13.0303(11)
b, Å	12.9228(15)	13.6954(11)
c, Å	23.830(3)	22.1635(18)
α, °	90	94.646(2)
β, °	96.596(3)	93.226(2)
γ, °	90	109.179(2)
V, Å^3	8610.5(18)	3708.9(5)
Z	4	2
Color, crystal shape	Colorless, block	Pale purple, block
Crystal size, mm	0.079 × 0.062 × 0.053	0.292 × 0.149 × 0.112
ρ_{calc}, g cm^{-3}	1.801	1.911
μ, mm^{-1}	2.074	2.880
Independent reflections (R_{int})	10242 (0.1132)	15662 (0.0504)
Reflections with $I > 2\sigma(I)$	6133	11626
Number of parameters	532	993
R_1 ($I > 2\sigma(I)$), wR_2	0.0762, 0.2361	0.0973, 0.2630
GOOF for F^2	1.057	1.161
T_{min}, T_{max}	0.6227, 0.9143	0.4935, 1.0000
ρ_{min}/ρ_{max}, e Å^{-3}	−2.084/2.403	−4.891/3.662

RESULTS AND DISCUSSION

An approach to the synthesis of polynuclear REE compounds is actively developed at present. The approach is based on controlled hydrolysis in the presence of organic ligands stabilizing a polynuclear hydroxo complex. The self-controlled hydrolysis can be performed due to using amines capable of acting simultaneously as both weak organic bases (reaction 1) and chelating ligands (reaction 2). The self-controlled character of hydrolysis is due to close basicity constants of Deta (pK_b = 3.8) and acidity of carboxylic acid (e.g., pivalic acid HPiv, pK_a = 5.0) and bringing out Deta from the reaction sphere upon the formation of chelate complexes. The simultaneous occurrence of hydrolysis and complex formation can result in the stabilization of the polynuclear hydroxo complexes (reaction 3) [17].

$$Ln(Tfa)_3 + xH_2O + x\text{Deta} \rightleftharpoons 1/m\left[Ln(Tfa)_{3-x}(OH)_x\right]_m + x(\text{DetaH})\text{Tfa}, \quad (1)$$

$$Ln(Tfa)_3 + n\text{Deta} \rightleftharpoons \left[Ln(Tfa)_3(\text{Deta})_n\right], \quad (2)$$

$$1/m\left[Ln(Tfa)_{3-x}(OH)_x\right]_m + n\text{Deta} \rightleftharpoons 1/m\left[Ln(Tfa)_{3-x}(OH)_x(\text{Deta})_n\right]_m, \quad (3)$$

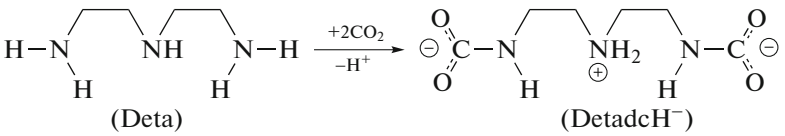

(4)

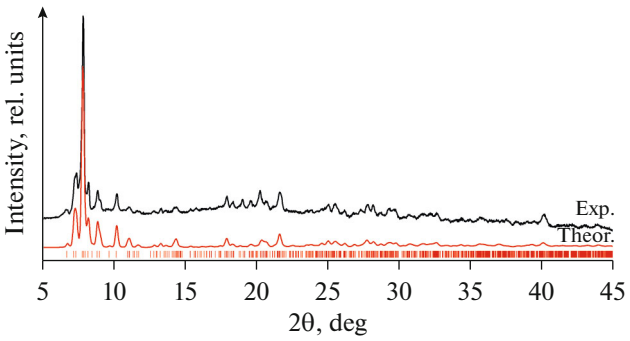

Fig. 1. Comparison of the XRD data for powdered compound **II** and theoretical X-ray pattern calculated from the crystal structure of compound **II**. Thermal expansion (a = 12.988(7), b = 13.950(8), c = 22.735(9) Å, α = 95.78(5)°, β = 92.75(4)°, γ = 109.48(6)°, V = 3849(4) Å^3) and the (00l) texture effects were taken into account. The calculated positions of the Bragg peaks are shown by vertical bars from the bottom.

In this work we studied the reactions of Deta with REE trifluoroacetates (salts of strong trifluoroacetic acid, pK_a = 0.5). Partial hydrolysis also occurs as a result of the slow crystallization of the reaction mixture in air. In this case, the degree of hydrolysis is lower than that in the case of pivalates, and molecular clusters with cubane core $Ln_4(OH)_4$ (one of the most abundant for REE carboxylates) are formed. A unique feature of the synthesis is the isolation of the crystalline compounds with the in situ formed diethylenetriamine-*N*,*N*'-dicarbamate anion (DetadcH$^-$) protonated at the central nitrogen atom. The formation of DetadcH$^-$ occurs due to CO_2 absorption from air by a solution of Deta (reaction 4) during the slow crystallization of the reaction mixture in an open beaker. It should be mentioned that DetadcH$^-$ is only one of a complicated set of products corresponding to different degrees of protonation and CO_2 addition [30, 31].

The degradation of aliphatic polyamines by the action of carbon dioxide and elevated temperature leading to the formation of various derivatives of urea and carbamic acid were described [32, 33]. According to our data, however, neither metal complexes with these dicarbamate ligands nor organic compounds containing a similar fragment were described up to presently. This is probably related to difficulties of synthesizing these compounds in the crystalline state. At the same time, the corresponding systems with polyamines are of interest from the viewpoint of their application in technologies in carbon dioxide trapping and storage [31, 34].

In this work we succeeded to isolate crystals of the compounds of two metals, lanthanum (**I**) and neodymium (**II**), containing, according to the XRD data, the cationic structural fragment of the same composition $[Ln_4(Deta)_4(OH)_4(Tfa)_3(DetadcH)_2]^{3+}$, out-of-sphere Tfa$^-$ anions, and water molecules.

The identity of the synthesized major product (powdered compound **II**) and the single crystals studied by XRD was confirmed by the coincidence of the experimental and theoretical powder XRD patterns (Fig. 1).

According to the XRD data, the most substantial difference between the structures of compounds **I** and **II** is that compound **I** crystallizes in the monoclinic $C2/c$ group, and axis 2 passes through the cationic $[Ln_4(Deta)_4(OH)_4(Tfa)_3(DetadcH)_2]^{3+}$ fragment (i.e., the symmetrically independent part contains half a cationic fragment), whereas compound **II** crystallizes in the triclinic group $P\bar{1}$, and the symmetrically independent part of the unit cell of compound **II** contains the full complex cation. In the structure of $[Ln_4(Deta)_4(OH)_4(Tfa)_3(DetadcH)_2]^{3+}$ four Ln atoms are localized at the vertices of the tetrahedron (Ln···Ln ≈ 4 Å), and four μ_3-OH groups that form the cubane metal–oxygen core $\{Ln_4(\mu_3\text{-}OH)_4\}$ are arranged above the tetrahedron faces at a height of 0.83–0.98 Å (Fig. 2). The compounds with the cubane core are widely described for *d* and *f* elements in both isolated molecular clusters [13, 14] and structural blocks of the more complicated polynuclear complexes [35, 36] and coordination polymers [37, 38].

The $[Ln_4(Deta)_4(OH)_4(Tfa)_3(DetadcH)_2]^{3+}$ complex cation contains Ln atoms of two types with different coordination environments (Fig. 3). The first type is presented by pairs of atoms La(1), La(1)^i in compound **I** and Nd(1), Nd(2) in compound **II** with the same-type coordination environment (three-capped trigonal prism, coordination number 9), which can reasonably be considered using Nd(1) as an example. The Nd(1) atom exists in the environment of three nitrogen atoms N(7)–N(9) of bichelate Deta, oxygen atoms O(1H)–O(3H) of three μ_3-OH groups, two oxygen atoms (O(1) and O(3)) of one bridging DetadcH$^-$, and one oxygen atom (O(9)) of bridging Tfa$^-$ (Table 2). The bridging Tfa$^-$ anion enters the coordination environment of Nd(2) by the second oxygen atom (O(10)).

The second type of Ln atoms is presented by the pairs La(3), La(3)^i in **I** and Nd(3), Nd(4) in **II** also with the same-type coordination environment (one-capped square antiprism, coordination number 9) considered for Nd(3) as an example. The Nd(3) atom is surrounded by three nitrogen atoms N(13)–N(15) of bichelate Deta, oxygen atoms O(2H)–O(4H) of three μ_3-OH groups, oxygen atoms O(4) and O(8) of two bridging DetadcH$^-$, and one oxygen atom O(13) of terminal Tfa$^-$ (Table 2). The terminal Tfa$^-$ anions form intramolecular hydrogen bonds with the μ_3-OH groups (Table 3).

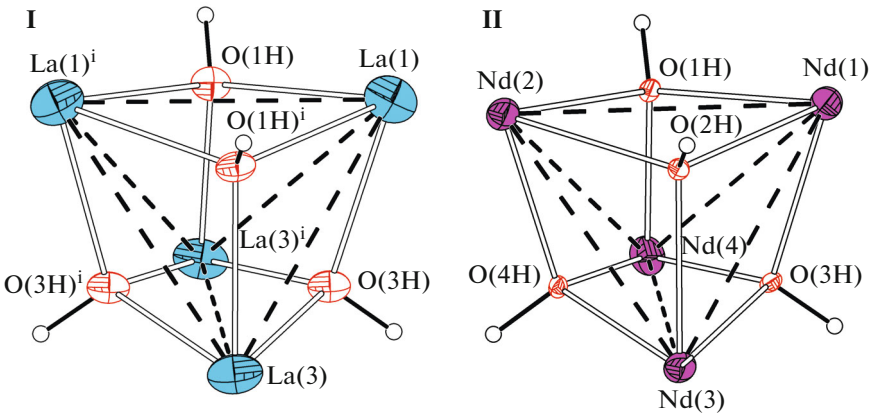

Fig. 2. Structure of the cubane metal–oxygen core in the tetranuclear complex cation $[Ln_4(Deta)_4(OH)_4(Tfa)_3(DetadcH)_2]^{3+}$ in the crystal structures of compounds **I** and **II**. Only the Ln atoms and μ_3-OH groups are shown for clarity. The edges of the Ln_4 tetrahedron are shown by dashed lines.

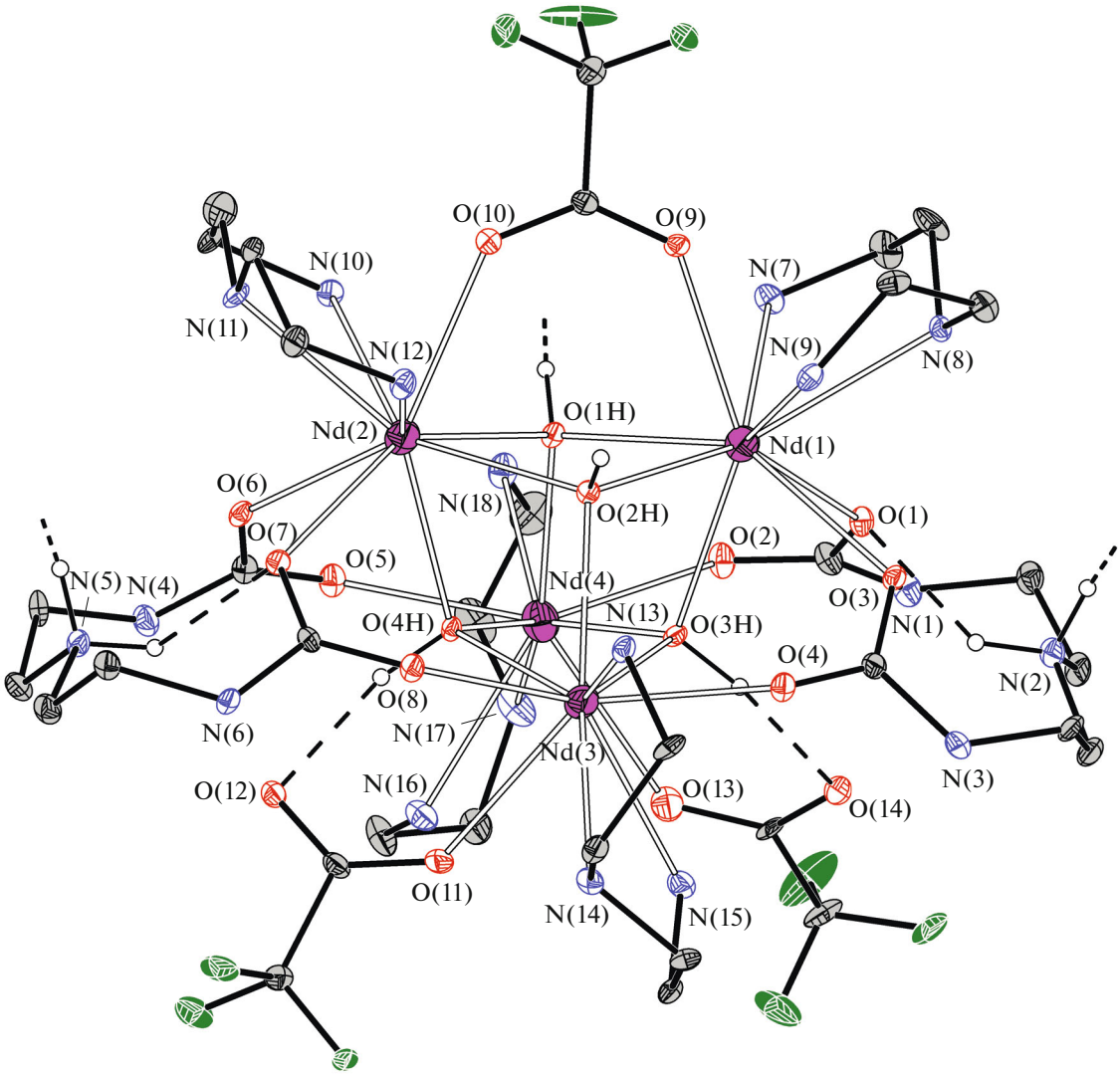

Fig. 3. Structure of the complex cation $[Nd_4(Deta)_4(OH)_4(Tfa)_3(DetadcH)_2]^{3+}$ in the crystal structure of compound **II**. Hydrogen atoms are omitted in part for clarity. Hydrogen bonds are shown by dashed lines.

Table 2. Interatomic distances (Å) in the complex cations $[Ln_4(Deta)_4(OH)_4(Tfa)_3(DetadcH)_2]^{3+}$ in the structures of complexes **I** and **II** according to the XRD data and DFT calculations

Bond Ln–L	Ln = La (**I**)		Ln = Nd (**II**)
	XRD	DFT	XRD
Ln(1)–O(1)	2.529(7)	2.611	2.456(10)
Ln(1)–O(3)	2.516(8)	2.562	2.541(12)
Ln(1)–O(1H)	2.538(8)	2.590	2.499(10)
Ln(1)–O(2H)	2.538(7)	2.573	2.474(8)
Ln(1)–O(3H)	2.498(6)	2.495	2.426(11)
Ln(1)–O(9)	2.590(8)	2.588	2.509(12)
Ln(1)–N(7)	2.719(10)	2.730	2.663(16)
Ln(1)–N(8)	2.733(11)	2.722	2.692(12)
Ln(1)–N(9)	2.751(11)	2.742	2.629(13)
Ln(2)–O(6)	2.516(8)	2.543	2.500(10)
Ln(2)–O(7)	2.529(7)	2.621	2.453(10)
Ln(2)–O(1H)	2.538(7)	2.572	2.493(8)
Ln(2)–O(2H)	2.538(8)	2.579	2.478(11)
Ln(2)–O(4H)	2.498(6)	2.497	2.421(11)
Ln(2)–O(10)	2.590(8)	2.599	2.535(12)
Ln(2)–N(10)	2.751(11)	2.732	2.642(17)
Ln(2)–N(11)	2.733(11)	2.726	2.688(13)
Ln(2)–N(12)	2.719(10)	2.743	2.681(15)
Ln(3)–O(4)	2.518(8)	2.561	2.432(11)
Ln(3)–O(8)	2.541(7)	2.613	2.424(9)
Ln(3)–O(2H)	2.533(6)	2.562	2.467(12)
Ln(3)–O(3H)	2.474(7)	2.513	2.459(9)
Ln(3)–O(4H)	2.502(8)	2.505	2.436(11)
Ln(3)–O(11)	2.626(9)	2.623	2.584(13)
Ln(3)–N(13)	2.713(9)	2.733	2.665(15)
Ln(3)–N(14)	2.722(9)	2.756	2.699(17)
Ln(3)–N(15)	2.720(9)	2.708	2.633(16)
Ln(4)–O(2)	2.541(7)	2.604	2.471(10)
Ln(4)–O(5)	2.518(8)	2.544	2.511(12)
Ln(4)–O(1H)	2.533(6)	2.550	2.456(11)
Ln(4)–O(3H)	2.502(8)	2.515	2.423(11)
Ln(4)–O(4H)	2.474(7)	2.520	2.434(9)
Ln(4)–O(13)	2.626(9)	2.634	2.639(17)
Ln(4)–N(16)	2.720(9)	2.709	2.679(16)
Ln(4)–N(17)	2.722(9)	2.759	2.684(17)
Ln(4)–N(18)	2.713(9)	2.726	2.63(2)

Note that both $DetadcH^-$ anions act only as bridging ligands, unlike four bichelate Deta, and the central nitrogen atom of $DetadcH^-$ is protonated and is not involved in coordination with the metal. Instead of this, the NH_2^+ group forms two hydrogen bonds (intramolecular and intermolecular).

In spite of the identical structure of the complex cation, compounds **I** and **II** differ in composition of the outer-of-sphere ligands, which explains the differences in symmetry of the crystal lattice. In the structure of compound **I**, one of the out-of-sphere Tfa^- anions and one HTfa molecule are disordered over two crystallographically equivalent positions with

Table 3. Parameters of the intramolecular hydrogen bonds O–H···O and N–H···O in the complex cations $[Ln_4(Deta)_4(OH)_4(Tfa)_3(DetadcH)_2]^{3+}$

D–H...A	Distance, Å			∠DHA, °
	D–H	H···A	D–A	
Ln = La (**I**)				
O(3H)–H(3)...O(14)	0.999	1.974	2.936	160.9
O(4H)–H(4)...O(12)	0.999	1.974	2.936	160.9
N(5)–H...O(7)	0.911	2.214	2.834	124.6
N(2)–H...O(1)	0.911	2.214	2.834	124.6
Ln = Nd (**II**)				
O(3H)–H(3)...O(14)	1.000	1.911	2.883	163.3
O(4H)–H(4)...O(12)	0.999	1.894	2.863	162.7
N(5)–H...O(7)	0.910	2.150	2.757	123.4
N(2)–H...O(1)	0.910	2.089	2.788	132.8

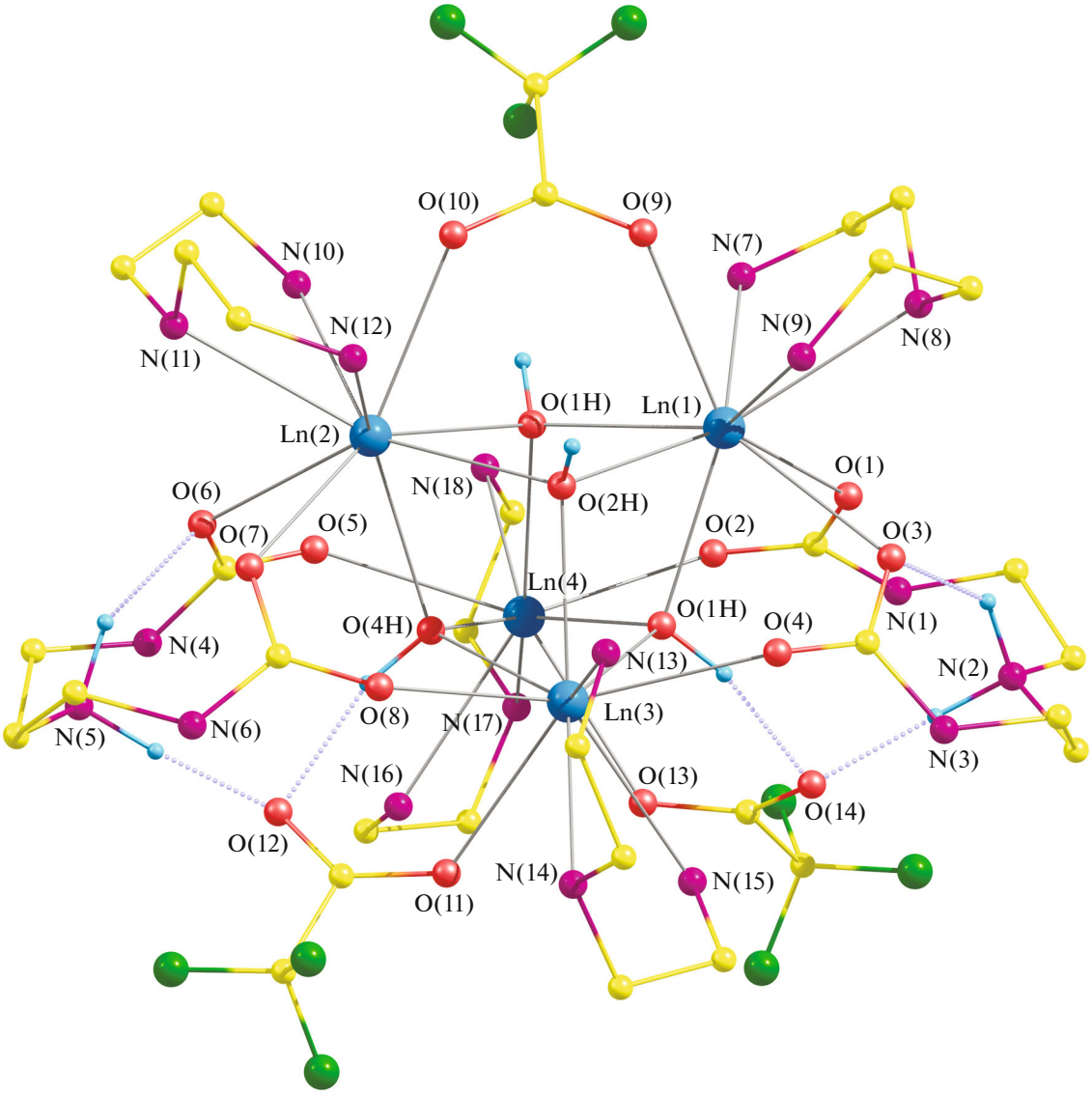

Fig. 4. Optimized geometry (DFT) of the complex cation $[La_4(Deta)_4(OH)_4(Tfa)_3(DetadcH)_2]^{3+}$. Hydrogen atoms are omitted in part for clarity.

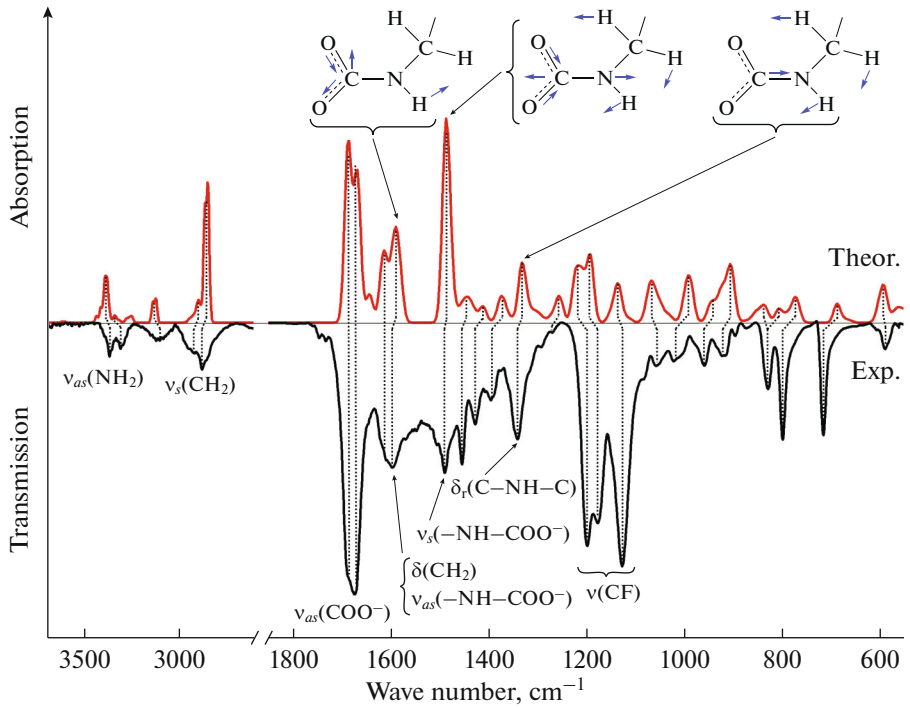

Fig. 5. Comparison of the experimental IR spectrum of compound **II** and theoretical (DFT) vibrational spectrum of the $[Ln_4(Deta)_4(OH)_4(Tfa)_3(DetadcH)_2]^{3+}$ cation. Normal vibration frequencies in the theoretical spectrum are presented with allowance for the scaling coefficients (0.93–0.95). The correspondence of the spectral bands is shown by dotted lines. The shapes of the normal vibrations involving the carbamate group are presented for the theoretical spectrum.

equal populations, while all out-of-sphere Tfa^- anions in the structure of compound **II** are ordered. The out-of-sphere water molecules forming a system of hydrogen bonds are located in cavities of the packing of the complex cations and anions.

The quantum chemical simulation of the isolated cationic $[La_4(Deta)_4(OH)_4(Tfa)_3(DetadcH)_2]^{3+}$ fragment showed a good agreement of the optimized geometry with the XRD results (Fig. 4), and the corresponding bond lengths differ by ca. 0.03 Å (Table 2). It should be mentioned that proton localization on the NH_2^+ groups and OH^- anions in the quantum chemical calculations also confirms the XRD results. The calculation of the frequencies and shapes of normal vibrations makes it possible to perform correct band assignments in the experimental spectrum (Fig. 5). The theoretical and experimental spectra are rather well consistent by both positions and band intensities. The high relative band intensities in a range of 1200–700 cm^{-1} in the experimental spectrum are associated with the out-of-sphere ligands that were not included in the calculation. According to the calculation data, the absorption bands at 1596, 1490, and 1339 cm^{-1} are related to vibrations of the carbamate groups, and their presence in the IR spectrum of powdered compound **II** additionally confirms the composition of this compound (Fig. 5).

To conclude, new molecular hydroxo complexes with the tetranuclear cubane core $\{Ln_4(\mu_3\text{-}OH)_4\}$ were synthesized by the controlled hydrolysis of La and Nd trifluoroacetates in the presence of diethylenetriamine. The reaction of diethylenetriamine with carbon dioxide in air during the synthesis resulted in the in situ formation of the anionic diethylenetriamine-*N*,*N*′-dicarbamate ligand incorporated in the complexes. The complexes with this ligand were isolated for the first time. The structures of the complexes were determined by XRD, and the quantitative and phase compositions were confirmed by a complex of methods: XRD, IR spectroscopy, and elemental analysis. The quantum chemical DFT calculations show a good agreement of the geometry of the complex with the XRD results, and the calculated vibrational spectrum corresponds to the experimental one additionally confirming the compositions and structures of the complexes.

FUNDING

Authors acknowledge the support from Lomonosov Moscow State University Program of Development.

This work was supported by the Russian Science Foundation, project no. 19-73-00277.

CONFLICT OF INTEREST

The authors declare that they have no conflicts of interest.

OPEN ACCESS

REFERENCES

1. D'Vries, R.F., Álvarez-Garcia, S., Snejko, N., et al., *J. Mater. Chem. C*, 2013, vol. 1, p. 6316.
2. Kreno, L.E., Leong, K., Farha, O.K., et al., *Chem. Rev.*, 2012, vol. 112, p. 1105.
3. Souri, N., Tian, P., Platas-Iglesias, C., et al., *J. Am. Chem. Soc.*, 2017, vol. 139, p. 1456.
4. Wang, W.-M., Li, X.-Z., Zhang, L., et al., *New J. Chem.*, 2019, p. 7419.
5. Guo, F.S., Leng, J.D., Liu, J.L., et al., *Inorg. Chem.*, 2012, vol. 51, p. 405.
6. Feng, L., Pang, J., She, P., et al., *Adv. Mater.*, 2020, vol. 66, p. 1.
7. Nikolaeva, A., Nygaard, R., Martynova, I., et al., *Polyhedron*, 2020, p. 114373.
8. Kendin, M. and Tsymbarenko, D., *J. Anal. Appl. Pyrolysis*, 2019, vol. 140, p. 367.
9. Kuzmina, N.P., Ibragimov, S.A., Makarevich, A.M., et al., *Chem. Mater.*, 2010, vol. 22, p. 5803.
10. Grebenyuk, D., Ryzhkov, N., and Tsymbarenko, D., *J. Fluorine Chem.*, 2017, vol. 202, p. 82.
11. Suzuki, Y., Nagayama, T., Sekine, M., et al., *J. Less-Common Met.*, 1986, vol. 126, p. 351.
12. Calvez, G., Le Natur, F., Daiguebonne, C., et al., *Coord. Chem. Rev.*, 2017, vol. 340, p. 134.
13. Wang, R., Liu, H., Carducci, M.D., et al., *Inorg. Chem.*, 2001, vol. 40, p. 2743.
14. Roitershtein, D.M., Vinogradov, A.A., Lyssenko, K.A., et al., *Inorg. Chem. Commun.*, 2017, vol. 84, p. 225.
15. Guo, P.H., Liu, J.L., Zhang, Z.M., et al., *Inorg. Chem.*, 2012, vol. 51, p. 1233.
16. Abbas, G., Lan, Y., Kostakis, G.E., et al., *Inorg. Chem.*, 2010, vol. 49, p. 8067.
17. Grebenyuk, D., Martynova, I., and Tsymbarenko, D., *Eur. J. Inorg. Chem.*, 2019, p. 3103.
18. Calvez, G., Daiguebonne, C., Guillou, O., et al., *Eur. J. Inorg. Chem.*, 2009, p. 3172.
19. Calvez, G., Guillou, O., Daiguebonne, C., et al., *Inorg. Chim. Acta*, 2008, vol. 361, p. 2349.
20. Wang, R., Zheng, Z., Jin, T., et al., *Inorg. Chem.*, 1999, vol. 38, p. 1813.
21. Langley, S.K., Chilton, N.F., Gass, I.A., et al., *Dalton Trans.*, 2011, vol. 40, p. 12656.
22. Datta, S., Baskar, V., Li, H., et al., *Eur. J. Inorg. Chem.*, 2007, p. 4216.
23. Andrews, P.C., Deacon, G.B., Frank, R., et al., *Eur. J. Inorg. Chem.*, 2009, p. 744.
24. Grebenyuk, D., Zobel, M., Polentarutti, M., et al., *Inorg. Chem.*, 2021, vol. 60, p. 8049.
25. Sheldrick, G.M., *Acta Crystallogr., Sect. C: Struct. Chem.*, 2015, vol. 71, p. 3.
26. Krause, L., Herbst-Irmer, R., Sheldrick, G.M., et al., *J. Appl. Crystallogr.*, 2015, vol. 48, p. 3.
27. Granovsky, A.A., *Firefly Computational Program Chemistry. Version 8.* http://classic.chem.msu.su/gran/firefly/index.html.
28. Dolg, M., Stoll, H., Savin, A., et al., *Theor. Chim. Acta*, 1989, vol. 75, p. 173.
29. Dolg, M., Stoll, H., and Preuss, H., *Theor. Chim. Acta*, 1993, vol. 85, p. 441.
30. Wong, M.K., Shariff, A.M., and Bustam, M.A., *RSC Adv.*, 2016, vol. 6, p. 10816.
31. Septavaux, J., Tosi, C., Jame, P., et al., *Nat. Chem.*, 2020, vol. 12, p. 202.
32. Thompson, J., Richburg, H., and Liu, K., *Energy Procedia*, 2017, vol. 114, p. 2030.
33. Wang, P., Fei, Y., Li, Q., et al., *Green Chem.*, 2016, vol. 18, p. 6681.
34. Poisson, G., Germain, G., Septavaux, J., et al., *Green Chem.*, 2016, vol. 18, p. 6436.
35. Zhou, Y., Zheng, X.Y., Cai, J., et al., *Inorg. Chem.*, 2017, vol. 56, p. 2037.
36. Ma, X.-F., Wang, H.-L., Zhu, Z.-H., et al., *Dalton Trans.*, 2019, vol. 48, p. 11338.
37. Zhou, J., Yan, S., Yuan, D., et al., *CrystEngComm*, 2009, vol. 11, p. 2640.
38. Cheng, J.W., Zheng, S.T., Liu, W., et al., *CrystEngComm*, 2008, vol. 10, p. 1047.

Translated by E. Yablonskaya